International Journal of Pharmaceutics 569 (2019) 118581

Contents lists available at ScienceDirect

International Journal of Pharmaceutics

journal homepage: www.elsevier.com/locate/ijpharm

Feasibility study into the potential use of fused-deposition modeling to manufacture 3D-printed enteric capsules in compounding pharmacies

Christoph Nober[a], Giuseppe Manini[a], Emeric Carlier[a], Jean-Marie Raquez[b], Samira Benali[b], Philippe Dubois[b], Karim Amighi[a], Jonathan Goole[a,c,*]

[a] Laboratory of Pharmaceutics and Biopharmaceutics, Université libre de Bruxelles, Campus de la Plaine, CP 207, Boulevard du Triomphe, Brussels 1050, Belgium
[b] Laboratory of Polymeric and Composite Materials (LPCM), Center of Innovation and Research in Materials and Polymers (CIRMAP), University of Mons, Place du Parc 23, B-7000 Mons, Belgium
[c] FabLab ULB, Rue Fritz Toussaint 8, 1050 Ixelles, Belgium

ARTICLE INFO

Keywords:
3D printing
Enteric capsules
Fused deposition modeling

ABSTRACT

The purpose of this work was to investigate the feasibility to manufacture enteric capsules, which could be used in compounding pharmacies, by fused-deposition modeling. It is well-known that conventional enteric dip coating of capsules in community pharmacies or hospitals is a time-consuming process which is characterized by an erratic efficacy. Fused-deposition modeling was selected as a potential 3D printing method due its ease and low-cost implementation. Before starting to print the capsules, an effective sealing system was designed via a computer-aided design program. Hot melt extrusion was used to make printable enteric filaments. They were made of the enteric polymer, a plasticizer and a thermoplastic polymer, namely Eudragit® L100-55, polyethylene glycol 400 and polylactic acid, respectively. Riboflavine-5′-phosphate was selected as a coloured drug model to compare the efficacy of the 3D printed capsules to that of enteric dip coated capsules as they are currently produced in community pharmacies and hospitals. Different parameters of fabrication which could influence the dissolution profile of the model drug, such as the layer thickness or post-processing step, were studied. It was demonstrated that our 3D printed enteric capsules did not release the drug for 2 h in acid medium (pH 1.2). However, they completely dissolved within 45 min at pH 6.8 which allowed the release of a minimal amount of 85% w/w of drug as it was recommended by the European Pharmacopoeia 9th Edition for enteric products.

1. Introduction

In 2014, 46% of new FDA approved dosage forms were still for oral delivery, either capsules or tablets (CDER's, 2014 reports). A large number of drugs can achieve maximal pharmacological effect or limited unwanted side effects when they are released in the intestine (Charbe et al., 2017). In particular, many pharmaceutically active acid-labile compounds, such as antibiotics or proton pump inhibitors, are susceptible to degradation when exposed at low pH values before reaching the enteric region where they can be absorbed to reach the systemic circulation (Horn and Howden, 2005). Other oral-delivered drugs may provoke irritation of the gastric mucosa and should be, therefore, preferably shielded from the gastric environments until their release in the intestine (e.g. non-steroidal anti-inflammatory drugs) (Langman, 2003). In addition, some drugs need to specifically target a section of the intestine, such as chemotherapeutic agents for (colon) cancer treatment or for the treatment of intestinal bowel diseases such as ulcerative colitis or Crohn's disease (e.g. anti-inflammatory drugs; oral corticosteroids) (Prakash and Markham, 1999).

An enteric coating must be able to resist to acidic pH (e.g. gastric conditions), but they should dissolve upon contact with intestinal fluids. Enteric polymers have to be economical and nontoxic. The resulting film should be applied with ease without the need of high-cost equipment and must be continuous (Reddy et al., 2013).

The process of enteric coating of galenic preparations compounded in community pharmacies or hospitals is a time-consuming process. The most commonly used polymer is cellulose acetate phthalate (CAP) which must be dissolved in an organic solvent to be used in enteric dip coating of capsules. However, the use of organic solvents is not free of risk as they are easily flammable, toxic, harmful to the environment and residual traces can remain in the final product (Mostafa et al., 2011). Moreover, the efficacy of such coating method is considered to be

* Corresponding author at: Laboratory of Pharmaceutics and Biopharmaceutics, Université libre de Bruxelles, Campus de la Plaine, CP 207, Boulevard du Triomphe, Brussels 1050, Belgium.
E-mail address: jonathan.goole@ulb.ac.be (J. Goole).

https://doi.org/10.1016/j.ijpharm.2019.118581
Received 25 April 2019; Received in revised form 5 July 2019; Accepted 28 July 2019
Available online 29 July 2019
0378-5173/ © 2019 Elsevier B.V. All rights reserved.

erratic and may lead to potential therapeutic failure (Murthy et al., 1988).

3D printing, also referred as solid freeform fabrication (SFF) process, represents an elegant tool for designing simple, accurate, cheap, structured and tailored drug delivery systems (Goole and Amighi, 2016). Since the first SFF technique became available in the early '90s at MIT (Cambridge, MA) (Sach et al., 1993), several reports have been published on the use of 3D printing for medical applications. More recently, fused-deposition modeling (FDM) has received growing attention as, compared to other SFF techniques, it offers somehow the most immediate potential to unit dosage fabrication (Long et al., 2017).

In FDM, a molten thermoplastic polymer filament is carried on by two rollers, molten in a high temperature heating block, extruded through a nozzle and finally deposited onto a build plate where the molten matter quickly solidifies. The print head can move within the x- and y-axes whereas the platform, which can be thermostatically controlled, can move vertically on the z-axis, creating 3D structures layer-by-layer by fusing the layers together (Goyanes et al., 2017). For instance, typical parameters that should be properly controlled during a FDM process are the infill density, the speed of the extruder, the layer thickness and the temperature of both nozzle and building plate (Goyanes et al., 2014). It quickly appeared to be useful to develop an alternative manufacturing approach based on a combination of both hot melt extrusion (HME) to manufacture printable filaments and FDM (Pietrzak et al., 2015).

Indeed, Melocchi and co-workers demonstrated the possibility to develop printable filaments based on insoluble, enteric soluble and swellable/erodible polymers, which were used to print 600 µm thick disks. The same group concluded that those filaments may potentially be suitable for printing modified-release capsules (Melocchi et al., 2016). Using budesonide-loaded polyvinyl alcohol filaments, Goyanes et al. developed caplets containing 9 mg of budesonide using FDM 3D printer. However, these caplets had to be coated with an enteric polymer to get delayed-release properties (Goyanes et al., 2015). Later, they used HME and FDM to manufacture 3D printed tablets from enteric polymeric filaments. Nevertheless, they did not print hollow capsules (e.g. infill at 0%) as the lowest infill was fixed at 20% (Goyanes et al., 2017). Maroni et al. allowed developing a 3D printed multi-compartment capsular device for two-pulse oral drug delivery made of hollow compartments. However, as it was not the aim of their study, a complete development of standard hollow delayed-release 3D printed capsule was not described (Maroni et al., 2017). In 2018, Smith and co-workers described the development of a single wall capsule. However, the rounded shape of their device was not similar to the dome of a standard capsule (Smith et al., 2018).

Therefore, to our knowledge, there is no study that has demonstrated the ability to manufacture 3D-printed standard-shape capsules capable of meeting the European Pharmacopoeia 9th Edition requirements for enteric-release oral dosage forms (no release of the drug into acidic medium at pH 1.2 for 2 h and at least 80% of dissolution within 45 min at pH 6.8). Riboflavin-5′-phosphate sodium (RF5′PNa) was used as a model drug due to its ease of quantification by spectrophotometry as well as for safety reasons. Such 3D-printed enteric capsules could be used in community pharmacies instead of using the erratic and time-consuming commonly used dip coating as well as to easily adapt the volume of the capsules (e.g. dedicated to the young patients) and the subsequent dose of drug.

2. Materials and methods

2.1. Materials

Polylactic acid (PLA) was purchased as extruded filaments from Makerbot® (1.75 mm diameter, print temperature 220–240 °C, $\rho = 1300\ kg/m^3$ MakerBot® Inc., USA) and NatureWorks® LLC ($\rho = 1240\ kg/m^3$, MFI = 6 g/10 min, 4.3 wt% D-isomer content). The enteric methacrylic acid copolymer Eudragit® L100-55 (EL) was purchased from Evonik™ (Darmstadt, Germany) and CAP was obtained from Sigma-Aldrich® (USA). Both polyethylene glycol 400 (PEG400) (Merck®, Germany) and diethyl phthalate (DEP) (Sigma-Aldrich®, USA) were used as plasticizers. Gelatine capsules (#00) were purchased from Capsugel® (France). RF5′PNa (Certa®, Belgium) was used as a model drug; croscarmellose sodium (Ac-Di-Sol®, FMC, USA) was employed as the superdisintegrant and lactose 80 mesh (DMV International®, Netherlands) was used as a diluent.

2.2. Methods

2.2.1. Preparation of the enteric coated capsules by dip coating

The preparation of the enteric coated capsules by dip coating was performed according to standard protocol that is currently used in community pharmacies and hospitals (Yang et al., 2018). Briefly, both CAP (8 g) and DEP (2 g) were dissolved in 90 g of a mixture of isopropanol and ethyl acetate (1:1) (VWR Chemical®, France). The dispersion was placed under magnetic stirring until complete dissolution. The fully-sealed gelatine capsules were immersed up to half the length in the solution, for 10 s, using a Pro-coater base kit with #00 holder (Torpac®, USA), removed and left to air dry during 15–20 min until the solvent had been evaporated. Similar procedure was done with the other half of the capsules. The process was repeated in triplicate to get homogenous coating.

2.2.2. Preparation of filaments

PLA which was purchased in the form of a filament was cut into small pieces. Thereafter, EL was added and, eventually, the required amount of PEG400 was dispersed in a mortar. Then, liquid nitrogen was poured over the viscous mass, which became very brittle. After crushing with a pestle, the fragments were passed through a 2.00 mm mesh sieve until reaching a coarse-grained "powder", which enabled an easy and continuous extruder feeding. Before HME, the mixture was stored in a desiccator overnight at 25 °C. Filaments were prepared by HME using a parallel twin-screw extruder (Thermo Scientific® Process 11, Thermo Fisher Scientific Inc.®, USA) with 7 separate heating zones, excluding the die (ø = 1.70 mm). Temperature, die pressure, torque and speed of rotation of the screws were continuously monitored. The speed of the screws was fixed at 10 rotations per minute (rpm) and each heating zone, including the die, was set at 150 °C, except for the first heating zone, which was heated up to only 140 °C. The filaments were manually pulled. To ensure that the extruded filaments were homogenous, a couple of extrusion cycles were conducted. The first extrudate was cut into small pieces before being extruded again. After production, the diameter of the filaments was checked every 5 cm in length with an digital calliper and portions that had not a diameter in the acceptable range of 1.70 ± 0.1 mm were discarded.

2.2.3. Capsules geometry

1,2,3 Design® (Autodesk®, USA) was used as the computer aided design (CAD) program to draw the capsules and to export them as .stl files. Three different sizes of capsules were evaluated (Table 1) and an effective sealing system was designed to enable to prevent the early release of the drug in acidic medium. The selected sizes of the capsules are those that are usually used in community pharmacies and hospitals.

Table 1
Dimensions (mm) of capsules #000, 00 and 0 (ANSM, 2017).

	000	00	0
Capsule length when closed (mm)	26.1	23.3	21.7
Body length (mm)	22.2	20.2	18.4
Head length (mm)	12.9	11.7	10.7
Body diameter (mm)	9.5	8.2	7.3
Head diameter (mm)	9.9	8.5	7.6

2.2.4. Fused deposition modeling

FDM was performed on a MakerBot® Replicator 2 equipped with a 0.4 mm nozzle (MakerBot® Industries, USA). The MakerBot® Desktop Beta Version 3.10.0.1364 Software was used as the slicer program with modified settings. For each 3D printing, at least 15 cm of the enteric filaments were used. Three thicknesses of layer were evaluated: 100, 200 and 300 µm. The optimal printing temperature was set at 167 °C, 172 °C and 175 °C for a layer thickness of 100 µm, 200 µm and 300 µm, respectively. Active cooling was activated at layer 3 or at layer 7, when a raft was needed, to accelerate the cooling of these layers as it was visually and empirically observed that, without this, the structure began to subside at these two specific layers. The fan power was fixed at 100%, 70% and 10% for a layer thickness of 100, 200 and 300 µm, respectively. The print speed corresponds to the speed of the nozzle during the printing process. It was set at 5 mm/s for a layer thickness of 100 and 200 µm. It was decreased to 3 mm/s for the 300 µm setting. The print speed of the dome was reduced to 2 mm/s and 1 mm/s for a layer thickness of 200 µm and 300 µm, respectively. The infill density was fixed at 0%, which allowed the printing of hollow capsules with one shell. The thickness of the domes was set at 400 µm. A raft was used to print the heads of the capsules. The air relative humidity and the temperature in the operating room were equilibrated at 30 ± 2% and at 20 ± 2 °C, respectively. Some 3D-printed capsules were put into a climate chamber at 45 °C or 60 °C for 10 to 15 s to evaluate the impact of post-proceeding heat treatment on the final release profiles of RF5′PNa. Indeed, one of the main disadvantages of FDM is linked to the seam lines forming between every two adjacent strands which inherently causes high surface roughness, or even weak adhesion between two layers. Post-proceeding heat treatment is known to improve the surface roughness of the FDM parts as well as to increase the adhesion between adjacent layers (Nguyen and Lee, 2018). Blue tape was used on the building plate to increase the adhesion of the first printed layer.

The 3D printer was cleaned after each printing session. To clean the heating block, its temperature was fixed at 250 °C for 5 min; the material remaining at the surface of the nozzle was removed with a brass brush; then, the nozzle was unscrewed and any residue was manually removed; finally, it was immersed in acetone for 5 min and phosphate buffer pH 6.0 for another 5 min before being dried under a hot air stream. The level of the build plate was checked after the cleaning.

2.3. Preformulation studies

2.3.1. Differential scanning calorimetry

Differential scanning calorimetry (DSC) analyses were recorded using a heat-flux type DSC Q2000 (TA Instruments®, USA) equipped with a cooling system. Nitrogen gas was used as purge gas (flow rate = 50 mL/min.) and data were collected with TA Instruments Universal Analysis 2000® software. Samples of 5–8 mg were introduced into aluminium pans and sealed with a lid made of the same material to evaluate the thermodynamic properties of the PLA as well as of the filaments. The reference specimen consisted of an empty sealed pan. During the first cycle, the oven was equilibrated at 0 °C for 5 min. Then, it was heated up by 20 °C/min to 200 °C. During the second cycle, it was cooled down to 0 °C. The parameters of the third cycle were similar to those of the first cycle.

2.3.2. Thermogravimetric analysis

Thermogravimetric analyses (TGA) were performed on a TGA Q500 (TA Instruments®, USA), equipped with a balance with a sensitivity of 0.1 µg. Nitrogen gas was used as purge gas (flow rate = 50 mL/min.). Samples of 5 to 8 mg were loaded into a platinum pan to evaluate the temperature of degradation (loss in mass) of the pure materials as well as the blends. The climatic chamber was equilibrated at 35 °C for 5 min. Then, it was heated up by 10 °C/min to 250 °C. The thermal degradation profile was analysed using the TA Instruments® Universal Analysis 2000 software.

2.3.3. Gel permeation chromatography

An Agilent® liquid chromatograph (Agilent Technologies, Inc., United States) equipped with an Agilent® degasser, an isocratic HPLC pump (flowrate = 1 mL/min.), an Agilent® autosampler (loop volume = 100 µL, solution concentration = 2 mg/mL), an Agilent® DRI refractive index detector and three columns: a PL® (Polymer Laboratories, Ltd., United Kingdom) gel 5 mm guard column and two PL® gel Mixed-B 5 µm columns (columns for separation of polystyrene with Mw ranging from 200 to 4×10^5 g/mol) were used at 30 °C to evaluate the molecular weight of PLA samples. $CHCl_3$ was used as mobile phase. Polystyrene standards were used for calibration.

2.4. In vitro evaluation of the 3D printed enteric hollow capsules

2.4.1. Optical microscopy

An Olympus® BX60 (Olympus® Corporation, Japan) optical microscope coupled on a JVC TK-C1381 (JVC®, Japan) camera was used to evaluate the thickness of the enteric coating as well as of the 3D printed enteric capsules.

2.4.2. Scanning Electron Spectroscopy

The surface of the printed capsules was visualized by Scanning Electron Spectroscopy (SEM) using a JSM-600 Scanning Electron Microscope (Jeol, Tokyo, Japan). They were fixed onto a carbon tape and coated with gold using a Balzers SCD 030 (Balzers Union Ltd., Liechtenstein).

2.4.3. Evaluation of the sealing of the 3D printed enteric capsules

Capsules # 0, 00 and 000 were printed using raw PLA filament. PLA which is an insoluble polymer widely used in FDM was selected as the printing material to be sure that the zone of contact between the body and the head of the capsule could be considered as the only cause of potential permeability. Therefore, if an early release of RF5′PNa appears in the acidic medium pH 1.2 with our enteric capsules, it will be assumed that the leak will come from a lack of control of the manufacturing parameters and not from the CAD model of the capsule.

The capsules were filled with 1% w/w of RF5′PNa, 30% w/w of crosscarmellose sodium and 69% w/w of lactose 80 mesh.

2.4.4. Dissolution tests

A Distek 2100C USP 29 dissolution apparatus (Distek Inc., North Brunswick, NJ, USA), according to Type II (paddle) method was used for the dissolution tests (37.0 ± 0.2 °C; 100 rpm). A sinker was used to kept the capsules at the bottom of the vessel. Dissolution tests were carried out in 900 mL of HCl 0.1 M (pH 1.2) for 2 h; then, the acidic medium was replaced by 900 mL of phosphate buffer 0.05 M (pH 6.8) for the next 45 min. As RF5′PNa is a photosensitive substance, the dissolution tests were performed in a dark room.

Dissolution was carried out on an equivalent of 13.0, 9.0 and 6.5 mg of RF5′PNa, from capsules #000, #00 and #0, respectively. The capsules were manually filled with respective amount of RF5′PNa, 30% w/w of crosscarmellose sodium and lactose 80 mesh ad. 100% w/w. The amount of RF5′PNa released was detected spectrophotometrically with a Nanophotometer® NP80 (Implen®, Germany) at a wavelength of 445 nm. The percentages of drug release were measured at preselected time intervals and averaged (n = 3).

3. Results and discussion

3.1. Design of an hermetic sealing

In order to not affect the compliance of patients, the focus was set on the design of hermetic sealing, without an excessive overlapping of the head and the body of the capsule. Indeed, such overlapping could drastically decrease the compliance of the patients who could feel the edges of the capsule head. The sealing was designed to be as short as

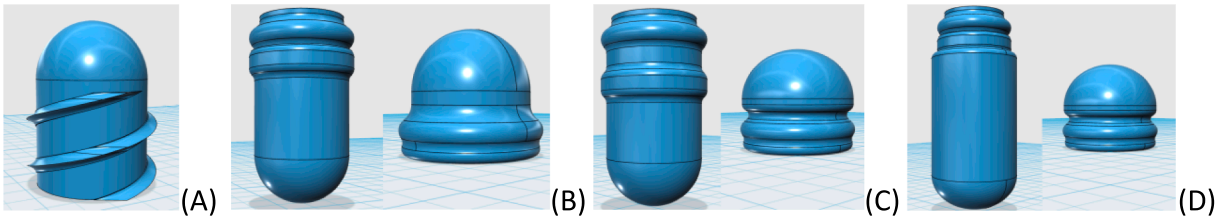

Fig. 1. Screw thread design of a capsule body (A), complete capsule designs (B–D) from 123 Design® (Autodesk®, USA).

possible and the thickness of the capsules was never thicker than one single shell. Although it is widely recognized that the main zone of weakness of capsules is located between their head and body, it was also demonstrated that the domes at both extremities as well as the permeability of the shell itself, may be considered as a secondary potential cause of water diffusion prior the dissolution of the capsule shell (McGinity and Felton, 2003). Therefore, in order to be sure that the zone of contact between the body and the head of the capsules could be considered as the only cause of the early penetration of the external medium, PLA, which is an insoluble polymer widely used in FDM, was selected as the printing material. In addition, the infill of both domes of the capsules was set at 100% for a thickness of 400 µm.

Four different designs were evaluated with the CAD program (Fig. 1A–D) according to the corresponding dimensions of capsules #000. Default settings of the slicer program were used with a layer thickness of 300 µm.

Due to a lack of resolution inherent to our 3D printer, the use of a screw thread to get an adequate sealing system had to be discarded. When using designs B and C, more than 20% w/w of RF5′PNa were released in the acidic medium (HCl 0.1 N pH 1.2) after 2 h. It has been assumed that a closure system lager than the body of the capsule did not allow achieving the desired sealing. In addition, this design did not prevent overlapping between the head and body of the capsule, even if it remained minimal (Fig. 1B&C). In contrast, a release of RF5′PNa lower than 5% w/w was observed in similar dissolution conditions when using design D (Fig. 1D). In that case, both head and body of the capsule were perfectly aligned.

As this very low percentage remained constant for 2 h, it was hypothesized that low residual amounts of RF5′PNa stuck onto the wall of the capsules during their manual filling. Therefore, the design was adjusted to comply with the outer dimensions of conventional capsules #000, 00 and 0 (Fig. 2) with similar sealing properties.

3.2. Composition of the enteric printable filaments

Eudragit® L100-55 was selected as the enteric polymer. It is widely used to coat dosage forms such as pellets, microspheres or granulates.

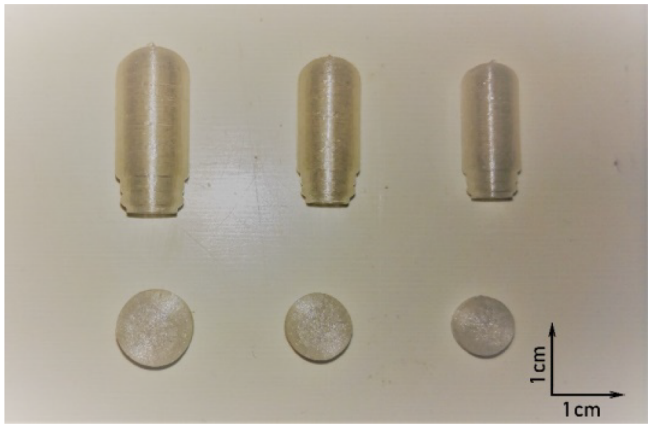

Fig. 2. PLA builds of the selected capsule design in different sizes (#000, 00, 0).

Moreover, its use in HME and FDM was already discussed in literature (Goyanes et al., 2015, 2017; Melocchi et al., 2016). EL is characterized by a glass transition temperature (Tg) of 111 °C (LaFountaine et al., 2016) and TGA has shown that it started to thermally degrade at 187 °C (data not shown). Preliminary trials have demonstrated that raw EL cannot be extruded without exceeding its degradation temperature was not possible due to high viscosity and sticking issues. To make the extrusion possible, plasticizers had to be incorporated as they can increase the free-volume between the polymer chains as well as the chain-mobility, which reduces the attraction between them. It was already observed that the concentration of plasticizer added to EL was inverse related to its Tg and its melt viscosity (LaFountaine et al., 2016). Therefore, the extrusion temperature, the torque and the die pressure could be reduced, which significantly improved the process of extrusion (Andrews et al., 2008).

It was found that a minimal amount of 20% w/w of triethyl citrate (TEC) should be added to allow extruding EL to obtain printable filaments without degradation of the polymer. Melocchi et al. had already succeeded in printing full disks (100% of infill) from mixtures based on the use of EL and TEC. (Melocchi et al., 2016). However, Qiao et al. have shown that PEG400 allowed a more efficient reduction of the Tg compared to TEC, at a same blend percentage with EL (Qiao et al., 2013). Moreover, our preformulation studies having shown that PEG 400 did not thermally degrade before reaching 194 °C (TGA data not shown), this plasticizer was selected to produce our enteric printable filaments.

Smooth filaments, characterized by proper diameters, were produced using 10, 15 and 20% w/w of PEG 400. However, filaments containing only EL and PEG 400 were all characterized by a very poor printability. Indeed, the adhesion to the built plate was impossible at printing temperatures from 150 °C to 180 °C, regardless the presence of a raft or blue tape and the printing speed. Therefore, it was decided to add PLA in the final blend to obtain a higher melt-strength of the filament during its melting inside the print head. Moreover, without the use of PLA, there was no adhesion on the build plate as well as between layers. PLA was also selected as it is a biocompatible and biodegradable polymer, which is FDA approved for human use.

However, although some physicochemical properties of PLA from NatureWorks® were available, almost nothing was found about that from Makerbot®. Therefore, their thermal properties as well as their molecular weight (Mw) and number average molecular weight (Mn) had to be firstly evaluated. TGA has shown that both PLA from NatureWorks® and MakerBot® started to degrade far above the degradation temperature of EL, namely at 270 °C and 288 °C, respectively. DSC analysis showed that the Tg of both samples were similar at 58 °C (Fig. 3). However, in contrast to that from Makerbot®, PLA from NatureWorks® was characterized by an exothermic peak at 98 °C which corresponded to its crystallization temperature. Since only crystallized material possesses a melting temperature (Tm) (Bhusnure, 2016), it was concluded that PLA from NatureWorks® had a higher crystalline content than that from Makerbot® which explained why its melting point peak was higher and more pronounced.

Indeed, T_m considerably varied between both PLA samples. As the T_m rises proportionally to the Mw of a polymer (Riga and Collins, 2006), it could be hypothesized that PLA chains from NatureWorks®

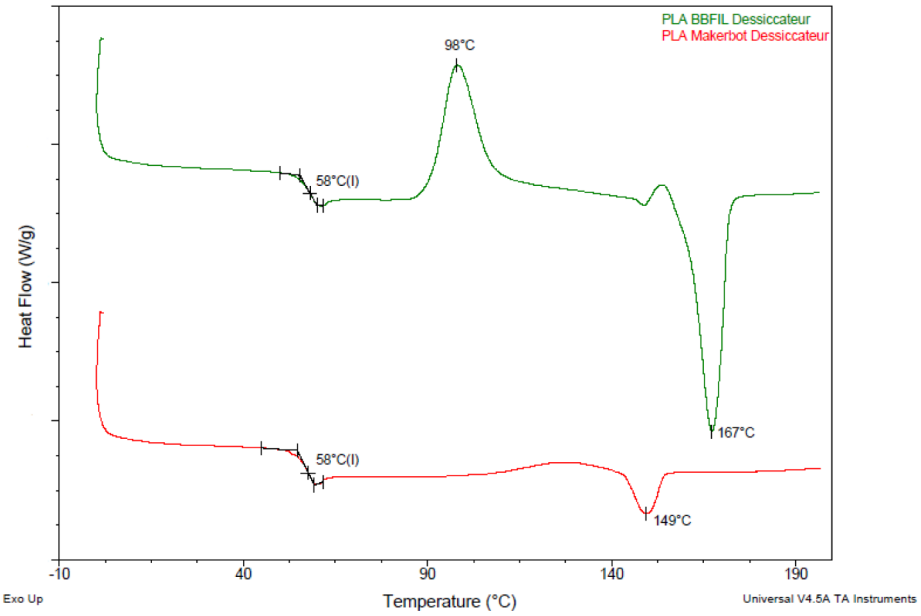

Fig. 3. DSC profiles of PLA from NatureWorks (green curve) and MakerBot® (red curve) obtained from the third cycle. (For interpretation of the references to colour in this figure legend, the reader is referred to the web version of this article.)

Table 2
Gel permeation chromatography analysis (Mw = Molecular weight), (Mn = Number average molecular weight).

Samples	Mw (g/mol)	Mn	Mw/Mn
MakerBot®	237,570	97,170	2.44
NatureWorks®	200,440	79,778	2.51

were most likely longer. Therefore, a gel permeation chromatography was carried out to evaluate the Mw of the different PLA samples (Table 2).

These results showed that the weight-average M_w of MakerBot® PLA was 18.5% higher than that from NatureWorks®, and that the Mn was 21.8% higher. Therefore, the higher T_m of PLA from NatureWorks® could not be explained by a higher M_w. Hence, the lower T_m of the MakerBot® PLA should be due to a higher D-isomer content (Auras et al., 2010). According to these data, a homogenous ternary blend filament could be extruded at a lower extrusion temperature with PLA from Makerbot® as it was characterized by a lower T_m than that from NatureWorks®, thereby reducing the risk of a thermal degradation of the blend.

EL being hygroscopic (Mwesigwa and Basit, 2016), the ternary blend was found to be sticky and cohesive if used immediately after blending. TGA showed a loss a weight of 4% w/w between 35 °C and 180 °C (data no shown). The poor melt-strength of the mixture prevented a homogenous distribution in the extruder. TGA demonstrated that the storage of the mixture in a desiccator overnight at 25 °C allowed water desorption and improved the feeding of the material during the HME process (Fig. 4). It seemed that a slight decrease of the moisture, from 4% w/w to 1% w/w was enough to improve the processability of the extrusion.

The ternary mix stocked at ambient air conditions started to lose mass at 85 °C. As the blend stored in a desiccator only started to lose mass at 187 °C, the lower thermal stability of the first mix was very likely due to the loss of water that the blend retained during storage.

3.3. Extrusion of filaments

The addition of PLA in the composition of the enteric filaments improved the extrusion as well as the printing process. PLA being an insoluble polymer, it was decided to reduce as much as possible its amount to not delay the dissolution of the 3D printed capsules at pH 6.8. The lowest percentage of PLA conferring a sufficient suppleness was found to be 10% w/w. At lower concentrations, the filaments were too brittle. They were also characterized by poor printability as they broke during the process and the layers did not adhere to each other. The ratio EL:PEG400 was fixed at 8:2 and PLA was added to this mixture in at 9:1 (Table 3).

As it has been shown by DSC and TGA, filaments containing PLA from MakerBot® were more easily extruded than those with PLA from NatureWorks®. Indeed, to obtain homogenous filaments with the second derivative of PLA, the extrusion temperature needed to be increased up to 170 °C (the T_m of PLA from NatureWorks® and Makerbot® was 167 °C and 149 °C, respectively (Fig. 3)). The resulting filaments presented a slightly yellowish aspect which probably corresponded to the beginning of thermal degradation of EL due to the high extrusion temperature as well as a long residence time inside the extruder.

The extrusion parameters were fixed when the torque remained stable during the whole process. The extrusion temperature was set 150 °C, except for the first heating zone which was heated at 140 °C. The temperature of the extruder needed to be high enough to process the blend forward, but not too high to not cause thermal degradation. It was observed that the use of an extrusion temperature lower than 150 °C drastically decreased the material flow inside the extruder due to a higher viscosity (visually observed). This drastically increased the internal pressure which could lead to the sudden stop of the extrusion process. The first heating zone was heated at lower temperature to avoid the clogging of the feed hopper which could be induced by the sticking of the powder on the walls of the hopper.

The extrusion speed was fixed at 10 rpm. Indeed, extrusion at higher speed resulted in die swell phenomenon. This phenomenon, which may also be more correctly called extrudate swell, is a result of the extensional rheology of the polymer melt and is attributed to the memory effect that the polymer melt experiences during flow (Alshetaili et al., 2016). Furthermore, because of the relatively low extrusion speed, the filaments went slower out of the die, facilitating the manual adjustment of the filament's diameter. However, TGA did not show any loss of weight when a sample was heated at 150 °C for 20 min (data not shown), which may significate that no thermal degradation may appear during the HME.

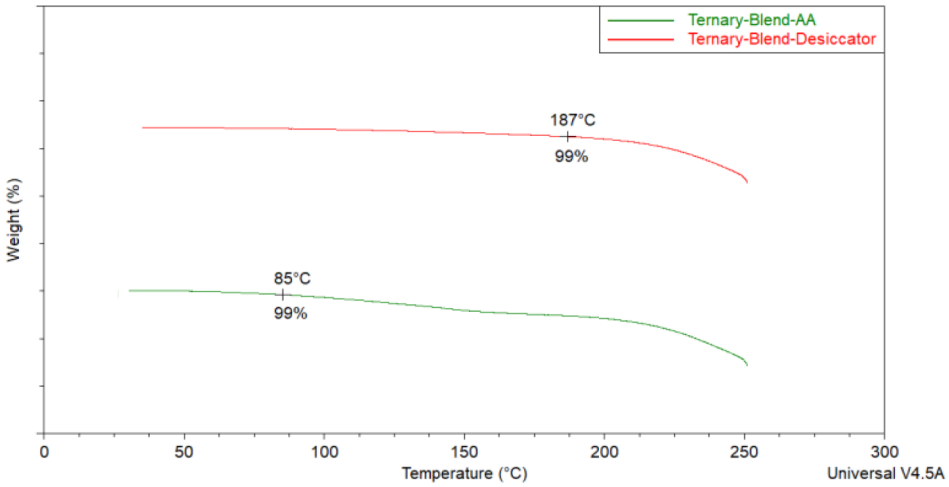

Fig. 4. TGA profiles of the ternary blend (EL:PEG400:PLA 72:18:10) stocked at 20 °C/50% of relative humidity (green curve) and at 25 °C in a desiccator (red curve) overnight. (For interpretation of the references to colour in this figure legend, the reader is referred to the web version of this article.)

Table 3
Composition of the ternary blend used to produce enteric printable filaments.

Components	Percentage (% w/w)
Eudragit® L100-55	72
PEG400	18
MakerBot® PLA Natural	10

The 3D printer was designed to be used with filaments characterized by a diameter of 1.70 mm. Only a minimal deviation of 0.1 mm could be tolerated. It was observed that greater deviation caused the filament to stop inside the print head. Indeed, it was previously demonstrated that the use of under-sized filaments may lead to the generation of air bubbles in the printed layers, whereas over-sized filaments may cause the blocking of the printer's drive mechanism (Melocchi et al., 2015). The extruded filaments were manually pulled on to obtain the targeted diameter. The oversized sections were discarded. The use of a spool on which the filament could be rolled up could allow an easier and better control over the diameter (Alshahrani et al., 2015).

To ensure that the compounds were homogenously dispersed inside the filaments, a couple of runs were conducted. However, as the speed of extrusion was relatively low, the influence of a second extrusion step on the thermal stability of the filaments was evaluated. DSC analysis demonstrated that the T_g of the filaments remained similar between the first and the second extrusion (data not shown), which may be considered as a proof of homogeneity (Qian et al., 2010). The T_m remained also similar at 147 °C.

Moreover, TGA demonstrated that the loss of mass started at 187 °C as it was observed from the blend before extrusion, regardless of the first or second cycle of extrusion (data not shown). Moreover, 187 °C corresponded to the beginning of the thermal degradation of pure EL. The ternary blend consisted of 72% w/w of EL, the low percentages of plasticizer and PLA did not influence the temperature of degradation of pure EL. Therefore, 187 °C has been considered as the highest temperature of the printing process that could be used.

3.3.1. 3D printing of the enteric capsules by FDM

The filaments were stored in a desiccator overnight at 25 °C prior to the printing process. In order to avoid the softening of the filaments during the printing process, it was observed that both temperature and relative humidity of the operating room must be properly controlled. They were fixed at 20 ± 2 °C and 30 ± 2%, respectively. Indeed, TGA demonstrated that, at higher values, filaments started to lose mass at temperatures lower than 100 °C which may be explained by the presence of water due to the hygroscopic properties of EL. The plasticizing effect of water on EL (Amighi and Moës, 1995) led to the softening of the filaments.

The filaments appeared to be very sensitive to the smallest changes of the printing temperature. A too high temperature caused collapse of capsules during the 3D printing as well as the generation of air pockets at their shell, which increased the risk of porosity and the loss of their gastro-resistance properties. In contrast, too low temperature caused a viscoelastic contraction of the capsules which led to lower adhesion between the layers.

It should also be mentioned that the increase of the layer thickness entailed higher flow of the matter which resulted in the need for a higher temperature for the printing process. The optimal temperatures were determined by printing several capsules and trail-and-error method. The optimal printing temperatures to be used when the layer thicknesses were fixed at 100, 200 or 300 µm were found to be 167 °C, 172 °C and 175 °C, respectively.

By default, the slicing program modulated the fan activity during the 3D printing workflow of each layer. Indeed, the fan activity was reduced for a short period of time during the deposition of the last part

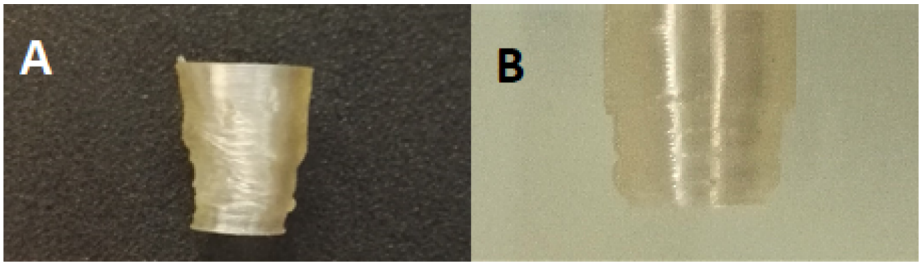

Fig. 5. Printed sealing system with activated fan modulation (A) and with constant fan activity (B).

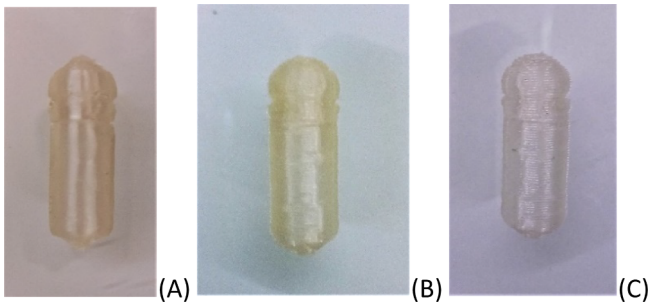

Fig. 6. 3D printed capsules #000 with a layer height of 100 µm (A), 200 µm (B) and 300 µm (C).

of each layer. This resulted in a decrease of the resolution which was detrimental to preserve the sealing between the head and the body of the capsule (Fig. 5A). The default settings from MakerBot® program were modified to deactivate the fan modulation and to obtain a constant fan activity, which allowed for a better resolution (Fig. 5B).

Once active cooling was set, the power of the fan was fixed according to the resolution of the 3D printed capsules. For a layer thickness of 100, 200 and 300 µm, the power of the fan was fixed at 100%, 70% and 10%, respectively. The power of the fan needed to be reduced to maintain optimal resolution when the layer thickness was increased. Indeed, layers characterized by lower thickness were reheated during the deposit of the next layer due to the passage of the print head. More efficient cooling was needed (higher power of the fan) to prevent slumping issues. In contrast, when the layer thickness increased, the nozzle had a larger distance to the previous one. Therefore, too much cooling would reduce the adhesion between the different layers as the previous layer was less reheated.

Layer thickness had the most important influence on the printing time of the capsules along with the printing speed and the minimum layer duration (MLD). As these parameters were also adapted according to the different resolution settings, the time to print did not vary linearly. For instance, to print a standard capsule #000, it took about 48, 18 and 17 min for a layer thickness of 100, 200 and 300 µm, respectively. A lower layer thickness resulted in a smoother surface of the capsules (higher resolution) and, as a result, the layers properly adhered to each other. Moreover, the capsules always showed a high level of details in terms of the sealing system. 3D printed capsules characterized by a higher layer thickness had a rougher surface. However, the details of the sealing system were always sufficient to guarantee its effectiveness.

Nevertheless, even when using the lowest layer thickness of 100 µm, compliance issues may occur due to the roughness of such 3D printed capsules compared to that from capsules that may be coated with the conventional dip method. Indeed, it was previously demonstrated that, in addition to the shape, density, and type of formulation, surface characteristics may affect the swallowability and oesophageal transit of capsules (and tablets), which may affect, or even reduce, patient compliance (Liu et al., 2014). Therefore, it seemed obvious that the use of more efficient 3D printers, offering a better resolution, should be considered to use such technology in compounding pharmacies.

Adequate resolution was achieved from printing speed of 5 mm/s for a layer thickness of 100 and 200 µm. For a layer thickness of 300 µm, the printing speed had to be decreased to 3 mm/s to improve the adhesion between layers, probably due to the slower speed of the print head which enabled a further re-heating of the previous layer.

For the printing of the domes, an infill of 100% was set for the first 0.40 mm. The print head as well as the filament passed from one side to the other above the hollow part of the capsule. The adhesion between the layers characterized by a thickness of 100 µm was strong enough to not have to reduce the printing speed during printing of the domes. To guarantee a good adhesion of the molten filament on the opposite part of the capsule when the thickness of the layers was greater than 100 µm, the printing speed was reduced to 2 mm/s for a layer thickness of 200 µm and to 1 mm/s for 300 µm. In general, it has been observed that the filament more easily follows the movement of the print head during its extrusion when the printing speed was reduced.

The MLD imposes the minimum printing time of each layer, which reduced the printing speed when the printing of a layer would have taken less time. The highest resolutions were obtained with MLDs of 10.0, 7.0 and 10.0 s for a layer thickness of 100, 200 and 300 µm, respectively. For a layer thickness of 100 µm, a higher MLD provided sufficient time to cool the previous layer, as active cooling was not sufficient to prevent sagging. For a layer thickness of 300 µm, a higher MLD probably provided adequate warming of the previous layer to achieve better adhesion.

The infill was set to 0%. The capsules had only one shell. The thinner the capsule is, the faster it will dissolve in the enteric environment (Mehuys et al., 2005). On the other hand, an overly thin capsule could consequentially have a higher permeability in acidic medium. Therefore, the standard printing nozzle with an effective diameter of 0.4 mm was selected instead of a reduced diameter nozzle. The dome was a critical part of the printing process as it was vulnerable to small holes due to the presence of overhang zones (Smith et al., 2018). The use of filled layers at this stage prevented the premature contact of the capsule's content with aqueous media. An infill of 100% was applied for the first 400 µm of the dome.

Better printing results were observed when the heads of the capsules were printed with the use of a raft. At a particular part of the sealing system, the diameter of the capsule's head quickly became narrower and then slowly wider again. This enabled the locking between the head and the body of the capsule. 3D printing of the dome with its convex

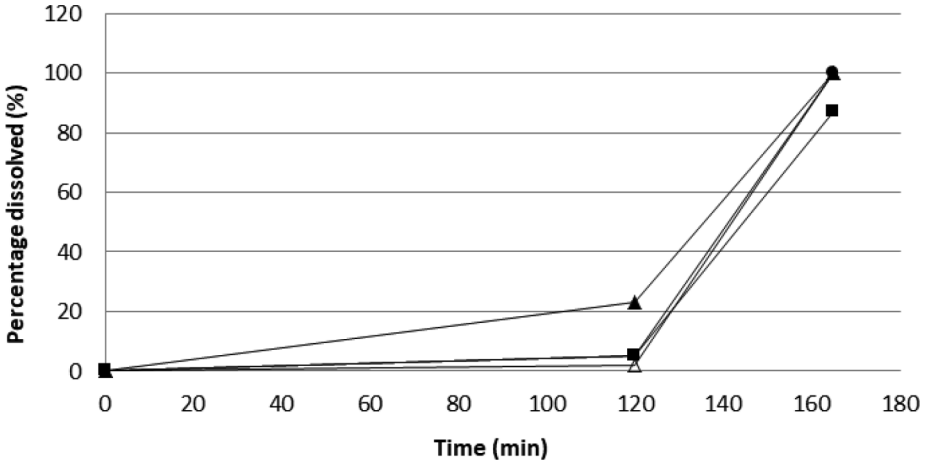

Fig. 7. Influence of the capsule #00's layer height 100 µm (■), 200 µm (●), 300 µm (▲) on the release profile of RF5′PNa, compared to the reference (Δ). The capsules were placed in HCl 0.1 N medium for 2 h, which was then replaced by a phosphate buffer pH 6.8 for 45 min (37 °C, 100 rpm). (n = 3).

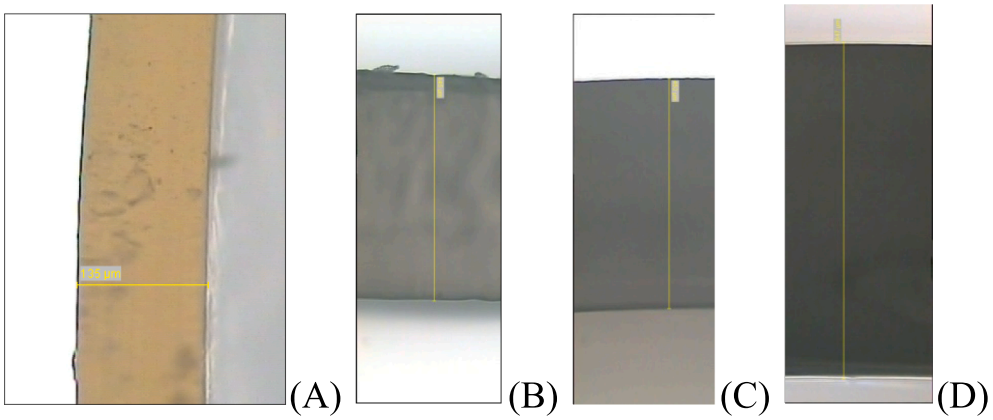

Fig. 8. Layer thickness of an enteric-coated capsule #00 and of the enteric printed capsules #000 with 100 µm setting (445 µm), 200 µm setting (452 µm) and 300 µm setting (647 µm).

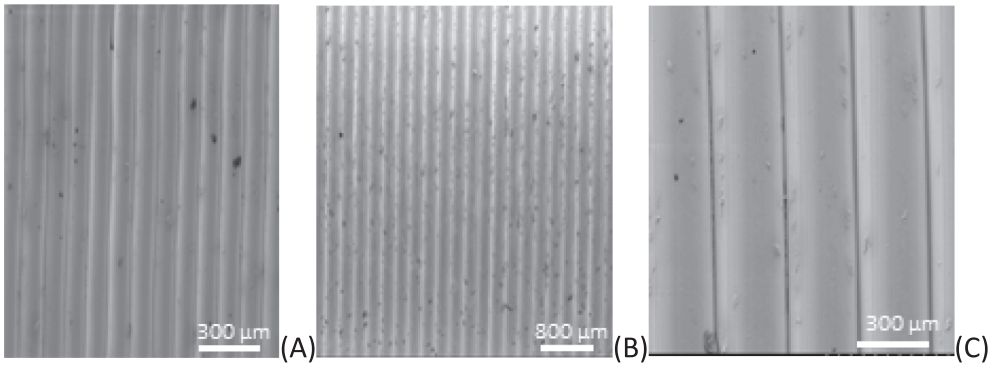

Fig. 9. SEM images from 3D printed enteric capsule #000 characterized by layers with 100 µm (A), 200 µm (B) and 300 µm (C) height.

part as the last part often resulted in the formation of a hole in the narrowing part of the sealing system due to the overhang zone. Indeed, the layer with a smaller diameter was less in contact with the previous one and the viscoelastic properties of the melted filament caused it to contract, potentially creating holes in its most convex part. When the dome was printed with its convex part as the first part, the sealing system was printed the other way around (the diameter first became slowly narrower to then subsequently quickly become wider again), and the emergence of holes could be avoided. Due to the viscoelastic properties, the 3D printing of the capsules becoming quickly wider was less problematic than thos being narrowed quickly. Active cooling was set at layer 3 or at layer 7 when a raft was needed, which allowed for a proper adhesion of the capsules on the built platform. These parameters being adjusted, high quality 3D printed capsules was obtained (Fig. 6A–C).

3.3.2. Dissolution tests

The dissolution profile of RF5′PNa from 3D printed enteric capsules were compared to that from conventional enteric dip-coated capsules #00. The capsules were manually filled with 1% w/w of RF5′PNa, 30% w/w of crosscarmellose sodium and 69% w/w of lactose 80 mesh. Dissolution was carried out on an equivalent of 9.0 mg of RF5′PNa. The influence of the layer thickness on the dissolution profile of RF5′PNa was evaluated on 3 D printed enteric capsules #00.

After 2 h in acidic medium (pH 1.2), no RF5′PNa was released from the coated capsules and 100% of the drug were released within 45 min in phosphate buffer pH 6.8.

3D printed enteric capsules released 5 ± 1% w/w of RF5′PNa when the layer thickness was set at 100 or 200 µm. Moreover, more than 80% w/w of RF5′PNa were released within 45 min in phosphate buffer pH 6.8 which was accordance with the European Pharmacopoeia 9th Edition criteria for oral enteric products (< 10% w/w). However, it could be interestingly noticed that the percentage of release was lower from 3D printed enteric capsules characterized by a layer thickness of 100 µm (87 ± 1% w/w) that that from those with a layer thickness of 200 µm (100 ± 1% w/w) (Fig. 7).

In contrast, 3D printed enteric capsules characterized by a layer thickness of 300 µm already released 23 ± 3% w/w after 2 h in HCl 0.1 N (pH 1.2) (Fig. 7)

Such high amount of release could only be due to an increased diffusion of water through the shell of the capsules. Mehuys and co-workers have previously demonstrated that the release of a drug could be slowed down by lowering the layer thickness, such decrease depending on the enteric polymer that was used (Mehuys et al., 2005).

Using optical microscopy, it was shown that the layer width was 445 and 452 µm for layer thickness of 100 µm and 200 µm, respectively. Both layer widths were lower than that from a layer thickness of 300 µm (647 µm). The layer width of all 3D printed enteric capsules was

Fig. 10. Impact of post-processing at a temperature higher than the Tg of 3D printed enteric capsule #000.

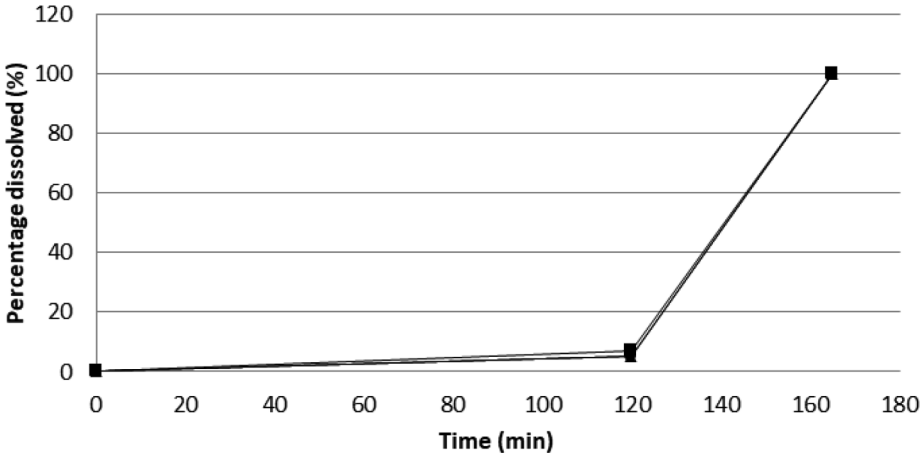

Fig. 11. Dissolution profile of RF5′PNa from 3D printed enteric capsules #0 (■), #00 (●), #000 (▲) characterized by a layer height of 200 µm. 2 h in HCL 0.1 N; 45 min in phosphate buffer pH 6.8.

found to be higher than that from the enteric dip-coated capsules (135 µm) (Fig. 8). The width of the layers having a thickness of 100 and 200 µm was in accordance with the diameter of the printing nozzle which was 0.40 mm. The upper layer width observed from layers characterized by a thickness of 300 µm could be explained by the fact that a larger amount of material had to leave the print head within the same period of time as that required for the 3D printing of layers characterized by smaller thickness (e.g. 100 µm and 200 µm). The time that was given to the polymers of the blend to relax and to orientate with the material flow was shorter, which could have resulted in a more significant die swell phenomenon. The use of a smaller printing nozzle could help to reduce the width of the printed layers. However, the 3D printed enteric capsules would be more vulnerable to printing irregularities and, as they have only one shell, a higher potential to leakage could arise from this due to melt-flow instability.

According Noyes-Whitney equation, the rate of dissolution should have been lower for 3D printed enteric capsules made of layers characterized by a thickness 300 µm as the distance of diffusion (the width of the layers) was higher than those from lower layer thickness. As our results did not correspond to the theory, it was thought that the lack adhesion between layers with a thickness of 300 µm could explain the higher release of RF5′PNa in acidic medium as water could diffuse more easily through the shell of the capsule. Moreover, the stronger adhesion between layers characterized by a thickness of 100 µm also explained the lower percentage of release at the end of the dissolution test (Fig. 7). As the layers characterized by lower thickness can be reheated and partially melt again during the deposit of the next layer due to the passage of the print head, the adhesion and the diffusion of water were stronger and lower, respectively.

SEM analysis demonstrated that the adhesion between layers of 300 µm thickness was clearly lower than that of layers with a thickness of 100 and 200 µm (Fig. 9). Therefore, for the 3D printed enteric capsules with a layer thickness of 300 µm, the enhancement of adhesion between the layers by post-processing heat-treatment was evaluated.

Chia et al. described that the extra sintering in an oven increased the strength of the printed objects (Chia and Wu, 2015). 3D printed enteric capsules #000 with a layer thickness of 300 µm were cured in an oven at a temperature above (60 °C) and below (45 °C) their Tg (55 °C) for 10 s. A post-processing heat treatment at 60 °C caused the printed circle to contract drastically (Fig. 10), a phenomenon already described by Chia et al. (Chia and Wu, 2015).

In contrast, when cured at 45 °C, no contraction was observed. However, the adhesion between the layers seemed to be improved as only 3 ± 1% w/w of RF5′PNa were released after 2 h in HCl 0.1 N (pH 1.2) instead of 23 ± 3% w/w without post-processing heat treatment.

Finally, the influence of the size of the 3D printed enteric capsules was evaluated using a constant layer thickness of 200 µm (Fig. 11). As it can be seen, the 3D printed enteric capsules satisfied the requirements of the European Pharmacopoeia 9th Ed. for the dissolution of enteric oral dosage form, regardless of their size. After 2 h in acidic medium pH 1.2, 3D-printed enteric capsules #0, #00 and #000 characterized by a layer thickness of 200 µm released 7 ± 2% w/w, 5 ± 2% w/w and 5 ± 1% w/w of RF5′PNa, respectively. Moreover, they were all able to release the entire amount of RF25′PNa within 45 min at pH 6.8.

4. Conclusion

It was possible to design a hermetic capsule closure system using a CAD program. Using a twin-screw extruder, printable filaments made of Eudragit® L100-55, PEG400 and PLA were produced. TGA and DSC analysis showed that the enteric filaments must be stored overnight in a desiccator at 25 °C to avoid breaking issues during the 3D printing process. It was shown that the default settings of printing from the program of MakerBot® must be modified to set a constant fan activity which allowed an activate cooling to get an optimal resolution of the 3D printed enteric capsules. A raft was needed during the 3D printing of the head of the capsules. Our 3D printed enteric capsules met the recommendations of the European Pharmacopoeia 9th Edition of oral enteric products, regardless of the layer thickness. However, capsules characterized by a layer thickness of 300 µm had to be cured at 45 °C for 10 s to enhance the adhesion between layers. As perspectives, it should be noticed that an alternative slicing program, which would enable the configuration of the printing speed per layer, would provide a better accuracy of the process. This would be especially useful to reduce printing issues encountered in the dome region. With higher precision, the width of the shell could be further reduced without sacrificing the uniformity of the capsules. Concerning the extrusion process, a belt conveyor system could contribute to extrude filaments with a more reproducible diameter, which would enhance the yield of the process as the fluctuation of matter leaving the nozzle would be reduced.

Declaration of Competing Interest

The authors declare that they have no known competing financial interests or personal relationships that could have appeared to influence the work reported in this paper.

Acknowledgments

The authors want to thank the Department of Materials engineering, characterization, synthesis and recycling (4MAT) from the Brussels School of Engineering (Faculty of Applied Sciences, ULB) (Dir. Prof. Godet, DelPlancke-Ogletree and Degrez), and especially M. Patrizio Madau, for having performed SEM analysis.

They also want to thank Victor Levy, Denis Terwagne and Alain Delchambre from the FabLab of ULB.

References

Alshahrani, S.M., Morott, J.T., Alshetaili, A.S., Tiwari, R.V., Majumdar, S., Repka, M.A., 2015. Influence of degassing on hot-melt extrusion process. Eur. J. Pharm. Sci. 80, 43–52.

Alshetaili, A.S., Almutairy, B.K., Alshahrani, S.M., Ashour, E.A., Tiwari, R.V., Alshehri, S.M., 2016. Optimization of hot melt extrusion parameters for sphericity and hardness of polymeric face-cut pellets. Drug Dev. Ind. Pharm. 42, 1833–1841.

Amighi, K., Moës, A.J., 1995. Evaluation of thermal and film forming properties of acrylic aqueous polymer dispersion blends: application to the formulation of sustained-release film coated theophylline pellets. Drug Dev. Ind. Pharm. 21, 2355–2369.

Andrews, G.P., Jones, D.S., Diak, O.A., McCoy, C.P., Watts, A.B., McGinity, J.W., 2008. The manufacture and characterisation of hot-melt extruded enteric tablets. Eur. J. Pharm. Biopharm. 69, 264–273.

ANSM, LGA certified – All about empty capsules [Online], Available: http://www.lga.fr/en/content/10-all-about-empty-capsules [accessed 05-15-2018].

Auras, R., Lim, L.-T., Selke, S., Tsuji, H., 2010. Poly(Lactic Acid): Synthesis, Structures, Properties, Processing, and Application. John Wiley & Sons Ltd, Hoboken, New Jersey, United States.

Bhusnure, O., 2016. Solid sample differential scanning calorimetry in biopharmaceutical discovery and development. World J. Pharm. Pharm. Sci. 5, 440–454.

Charbe, N.B., McCarron, P.A., Lane, M.E., Tambuwala, M.M., 2017. Application of three-dimensional printing for colon targeted drug delivery systems. Int. J. Pharm. Investig. 7, 47–59.

Chia, H.N., Wu, B.M., 2015. Recent advances in 3D printing of biomaterials. J. Biol. Eng. 9, 4–9.

Goole, J., Amighi, K., 2016. 3D printing in pharmaceutics: a new tool for designing customized drug delivery systems. Int. J. Pharm. 499, 376–394.

Goyanes, A., Buanz, A.B.M., Basit, A.W., Gaisford, S., 2014. Fused-filament 3D printing (3DP) for fabrication of tablets. Int. J. Pharm. 476, 88–92.

Goyanes, A., Chang, H., Sedough, D., Hatton, G.B., Wang, J., Buanz, A., Gaisford, S., Basit, A.W., 2015. Fabrication of controlled-release budesonide tablets via desktop (FDM) 3D printing. Int. J. Pharm. 496, 414–420.

Goyanes, A., Fina, F., Martorana, A., Sedough, D., Gaisford, S., Basit, A.W., 2017. Development of modified release 3D printed tablets (printlets) with pharmaceutical excipients using additive manufacturing. Int. J. Pharm. 527, 21–30.

Horn, J.R., Howden, C.W., 2005. Review article: similarities and differences among delayed-release proton-pump inhibitor formulations. Aliment. Pharmacol. Ther. 22 (Suppl 3), 20–24.

LaFountaine, J.S., McGinity, J.W., Williams, R.O., 2016. Challenges and strategies in thermal processing of amorphous solid dispersions: a review. AAPS PharmSciTech 17, 43–55.

Langman, M.J., 2003. Adverse effects of conventional non-steroidal anti-inflammatory drugs on the upper gastrointestinal tract. Fundam. Clin. Pharmacol. 17, 393–403.

Liu, F., Ranmal, S., Batchelor, H.K., Orlu-Gul, M., Ernest, T.B., Thomas, I.W., Flanagan, T., Tuleu, C., 2014. Patient-centred pharmaceutical design to improve acceptability of medicines: similarities and differences in paediatric and geriatric populations. Drugs 74, 1871–1889.

Long, J., Gholizadeh, H., Lu, J., Bunt, C., Seyfoddin, A., 2017. Application of fused deposition modelling (FDM) method of 3D printing in drug delivery. Curr. Pharm. Des. 23 (3), 433–439.

Maroni, A., Melocchi, A., Parietti, F., Foppoli, A., Zema, L., Gazzaniga, A., 2017. 3D printed multi-compartment capsular devices for two-pulse oral drug delivery. J. Control Release 28, 10–18.

McGinity, J.W., Felton, L.A., 2003. Enteric Film Coating of soft gelatin capsule. Drug Dev. Del. 3 open access.

Mehuys, E., Remon, J.-P.P., Vervaet, C., 2005. Production of enteric capsules by means of hot-melt extrusion. Eur. J. Pharm. Sci. 24, 207–212.

Melocchi, A., Parietti, F., Loreti, G., Maroni, A., Gazzaniga, A., Zema, L., 2015. 3D printing by fused deposition modeling (FDM) of a swellable/erodible capsular device for oral pulsatile release of drugs. J. Drug Deliv. Sci. Technol. 30, 360–367.

Melocchi, A., Parietti, F., Maroni, A., Foppoli, A., Gazzaniga, A., Zema, L., 2016. Hot-melt extruded filaments based on pharmaceutical grade polymers for 3D printing by fused deposition modeling. Int. J. Pharm. 509, 255–263.

Mostafa, H.F., Ibrahim, M.A., Mahrous, G.M., Sakr, A., 2011. Assessment of the pharmaceutical quality of marketed enteric coated pantoprazole sodium sesquihydrate products. Saudi. Pharm. J. 2, 123–127.

Murthy, K.S., Kubert, D.A., Fawzi, M.B., 1988. In vitro release characteristics of hard shell capsule products coated with aqueous- and organic-based enteric polymers. J. Biomater. Appl. 3, 52–79.

Mwesigwa, E., Basit, A.W., 2016. An investigation into moisture barrier film coating efficacy and its relevance to drug stability in solid dosage forms. Int. J. Pharm. 497, 70–77.

New Drugs at FDA: CDER's New Molecular Entities and New Therapeutic Biological Products 2014, Consulted on May 15th 2018.

Nguyen, T.K., Lee, B.-K., 2018. Post-processing of FDM parts to improve surface and thermal properties. Rapid Prot. J. 24, 1091–1100.

Pietrzak, K., Isreb, A., Alhnan, M.A., 2015. A flexible-dose dispenser for immediate and extended release 3D printed tablets. Eur. J. Pharm. Biopharm. 96, 380–387.

Prakash, A., Markham, A., 1999. Oral delayed-release mesalazine: a review of its use in ulcerative colitis and Crohn's disease. Drugs 57, 383–408.

Qian, F., Huang, J., Zhu, Q., Haddadin, R., Gawel, J., Garlise, R., Hussain, M., 2010. Is a distinctive single Tg a reliable indicator for the homogeneity of amorphous solid dispersion? Int. J. Pharm. 395, 232–235.

Qiao, M., Zhang, L., Ma, Y., Zhu, J., Xiao, W., 2013. A novel electrostatic dry coating process for enteric coating of tablets with Eudragit® L100–55. Eur. J. Pharm. Biopharm. 83, 293–300.

Reddy, B.V., Navaneetha, K., Reddy, B.R., 2013. Tablet coating industry point view - a comprehensive review. Int. J. Pharm. Biol. Sci. 3, 248–261.

Riga, A., Collins, R., 2006. Differential Scanning Calorimetry and Differential Thermal Analysis. John Wiley & Sons Ltd, Hoboken, New Jersey, United States.

Sach E.M., Haggerty J.S., Cima M.J., Williams P.A., 1993, Three-dimensional printing techniques, US Patent 5204055.

Smith, D.M., Kapoor, Y., Klinzing, G.R., Procopio, A.T., 2018. Pharmaceutical 3D printing: design and qualification of a single step print and fill capsule. Int. J. Pharm. 544, 21–30.

Yang, Y., Shen, L., Yuan, F., Fu, H., Shan, W., 2018. Preparation of sustained release capsules by electrostatic dry powder coating, using traditional dip coating as reference, Author links open overlay panel. Int. J. Pharm. 543, 345–351.